Engineering Structures 169 (2018) 1–14

Contents lists available at ScienceDirect

Engineering Structures

journal homepage: www.elsevier.com/locate/engstruct

Corrective countermeasure for track transition zones in railways: Adjustable fastener

Haoyu Wang*, Valeri Markine

Delft University of Technology, Delft, The Netherlands

ARTICLE INFO

Keywords:
Adjustable fasteners
Railway track modelling
Transition zone
Corrective countermeasures
Finite element method

ABSTRACT

Transition zones in railway tracks are the locations with considerable variation in the vertical stiffness of supporting structures. Typically, they are located near engineering structures, such as bridges, culverts, tunnels and level crossings. In such locations, the variation of the vertical stiffness and the differential track settlement result in amplification of the dynamic forces acting on the track. This amplification contributes to the degradation process of ballast and subgrade, ultimately resulting in the increase of maintenance costs.

The paper studies a corrective countermeasure that can mitigate the track degradation in transition zones when differential settlement appears. The countermeasure is the adjustable rail fastener and its working principle is to eliminate the gap under hanging sleepers by adjusting the shims (height of the fastener). The adjustable fasteners are first tested on three transition zones, wherein the adjusted heights of fasteners (accumulated voiding) are recorded after the 2-month and 5-month operation. The test results show the adjustable fasteners are effective to mitigate the track degradation in the transition zones. The effect of the adjustable fasteners on the dynamic behaviour of transition zones is analysed using the FE method. The results show that the adjustable fasteners are effective to reduce the amplification of wheel forces, achieve a better stress distribution in ballast, and decrease the normal stresses in rails in transition zones. Parametric studies are also performed to study the applicability of the adjustable fasteners.

1. Introduction

Transition zones in railway tracks are locations with considerable variation in the vertical stiffness of supporting structures. Typically, they are located near engineering structures, such as bridges and slab tracks. An example of a typical transition zone is shown in Fig. 1.

In those locations, the variation of the vertical stiffness together with the differential settlement of tracks (when the foundation settles unevenly) results in amplification of dynamic forces, which contributes to the degradation of ballast and subgrade, ultimately resulting in deterioration of the vertical track geometry or even the damage of track components. To keep track transition zones in operation, more maintenance is required as compared to free tracks [1,2]. For instance, in the Netherlands, the maintenance activities on the tracks in transition zones are performed up to 4–8 times more often than that on free tracks [3,4]. Transition zones in the other countries of Europe and the US also require additional maintenance [5,6].

Even though many countermeasures have been used in transition zones, severe track deterioration in transition zones is still often observed [7,8]. In [9], three countermeasures including geocell, cement, and hot mix asphalt were applied on three similar transition zones. Compared to a plain transition zone (no countermeasure is applied) as a reference, it has been found that all countermeasures were not sufficient to reduce the settlement in the transition zones. In [10], the countermeasure, which uses an approaching slab linking the ballast track onto a concrete culvert, 'has exacerbated rather than mitigated the (transition) problem'. These findings are in agreement with [11], where the authors indicated that 'the problem of track degradation associated with stiffness variations is far from being solved'.

According to the settlement behaviour of ballast tracks [12–17], the track settlement process can be divided into two stages (as shown in Fig. 2). Stage 1 is the rapid settlement process, caused by the volumetric compaction and abrasion of ballast particles. Stage 2 is the standard settlement process (until the end of the maintenance interval) caused by the frictional sliding of particles. The settlement of ballast, subballast, and subgrade in Stage 1 is: (1) fast, which happens only after few months; (2) large, accounts for approximately 50% of the total settlement in a maintenance interval; (3) somewhat inevitable, which happens even though it was compacted. On the contrary to the large settlement appearing in ballast tracks, the engineering structures barely

* Corresponding author.
E-mail address: H.Wang-1@tudelft.nl (H. Wang).

https://doi.org/10.1016/j.engstruct.2018.05.004
Received 16 December 2017; Received in revised form 25 April 2018; Accepted 2 May 2018
Available online 16 May 2018
0141-0296/

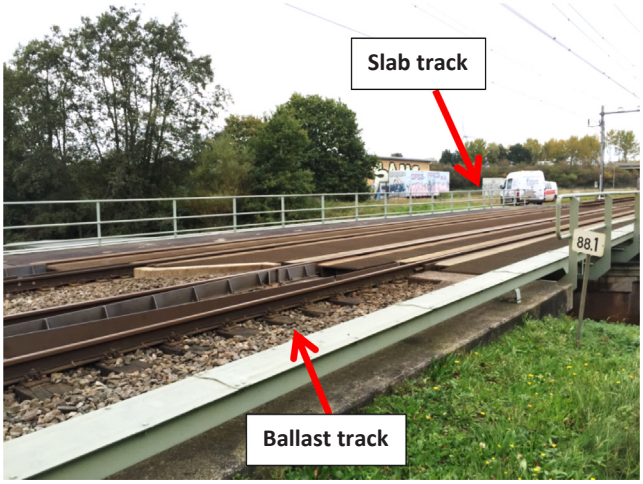

Fig. 1. Track transition zones.

settle, which creates a considerable geometry irregularity (differential settlement). After the differential settlement appears (corresponding to the beginning point of Stage 2, see Point B in Fig. 2), one end of the rails is settled together with the ballast track, while the other end is constrained by the engineering structures, creating gaps under sleepers (also known as hanging sleepers or voiding) on the embankment side.

Due to the existence of the gaps, the dynamic responses in transition zones are significantly increased [19,20]. For instance, a 1 mm gap can increase the sleeper-ballast contact force in adjacent locations by 70% [21]; and the 2 mm gap can lead to 85% increase of wheel forces [19]. It should be noted that the settlement curve in Fig. 2 is only for open ballast tracks. This is because the dynamic responses (e.g. wheel-rail interaction forces and ballast stress) are increased by the differential settlement and alter the settlement curve (mainly in Stage 2). An example of the transition zone with a large differential settlement is shown in Fig. 3 [18].

Therefore, the countermeasures can be categorized according to the settlement behaviour into the preventive countermeasures and corrective countermeasures. The preventive countermeasures are implemented during the construction prior to the track operation, while the corrective ones are used when the track has already settled (the differential settlement is visible). The studies of the transition zones with the perfect geometry, i.e. considering the beginning point of Stage 1 (Point A in Fig. 2), are more suitable for the preventive countermeasures, such as the studies in [8,22–27]; while for the analysis of corrective countermeasures, the numerical models have to take the differential settlement into account. The corrective countermeasures that can timely mitigate the transition zone problems caused by differential settlement (at Point B in Fig. 2) are required further studies.

This study focuses on the corrective countermeasures for transition zones which should meet the following requirements:

Fig. 3. Transition zone with a large differential settlement, from [18].

- The corrective operations should be performed in short track-possession windows manually or by using small machines.
- The corrective countermeasures should be able to mitigate the track degradation in transition zones.

The paper presents the experimental and numerical analysis of a corrective countermeasure – the adjustable fastener. The adjustable fastener intents to fill the partial gap between a sleeper and ballast by shims, whereas it prevents a large operation such as tamping. Even though (unloaded) track alignment is not restored, the hanging sleepers in the vicinity of engineering structures are eliminated, which can slow down the track degradation in transition zones.

The paper is organised as follows. The preventive and corrective countermeasures for transition zones are reviewed in Section 2, including the introduction of the adjustable fastener. The measurement results of three transition zones with the adjustable fasteners are discussed in Section 3. In Section 4, the dynamic behaviour of the transition zone (with differential settlement) with the adjustable fasteners is analysed using FE method. Finally, conclusions are given in Section 5.

2. Countermeasures for transition zones

The countermeasures for transition zones can be divided according to their application period, which is either the design stage (preventive measures) or the operation stage (corrective measures).

When designing a transition zone, the primary goal is to construct a zone with smooth changes of the vertical stiffness from the embankment to the engineering structure. A thorough review of the countermeasures for transition zones can be found in [28]. The countermeasures are applied to embankments or/and engineering structure. The intent of the countermeasures on the embankment is to reinforce the ballast track on different levels using various measures such as:

- Subgrade: the geocell, geotextile, cement, hot mix asphalt [9,29], and transition wedge (special backfill) [30];
- Ballast: the ballast glue [31], under ballast mat [32], pile or steel bar underneath the ballast [8,33], and ballast containment wall [34];
- Sleepers: sleeper modifications such as increasing its length and

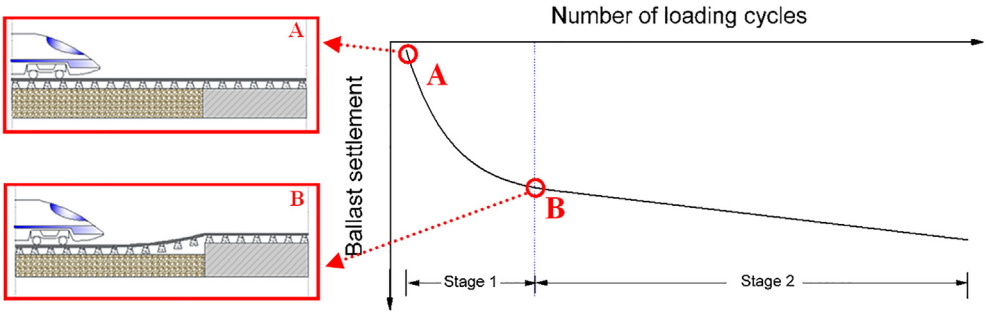

Fig. 2. Schematic permanent settlement curve of ballast as a function of loading cycles (only for open ballast tracks), from [18].

reducing the spacing [27,34] and weight [35,36].

The countermeasures on engineering structures are intended to decrease the stiffness of the tracks, for instance using rail pads [37], under slab pads [34] and under sleeper pads [24,25]. In addition, some countermeasures increase the intergrade stiffness of transition zones such as using auxiliary rails [27,34,36] and approaching slabs [38]. In some cases, a combination of several countermeasures is used [28].

When the preventive countermeasures do not mitigate the track degradation efficiently, e.g. [9,10], or no countermeasures are used, e.g. [7,39], critical differential settlement may appear in a maintenance cycle. The differential settlement may result in the damage of track components and deterioration of the passenger's comfort. To mitigate the existing differential settlement, the corrective countermeasures are necessary. Besides, the hanging sleepers also appear in the vicinity of the engineering structure (0.9 m [22] or 1.5 m [40] from the engineering structure). However, due to the abutment or the transition structure, it is not always possible for tamping machines to perform track maintenance near engineering structures. In these situations, corrective countermeasures that can be performed manually or by small packing machines can be applied. The general principle of the corrective countermeasures is to fill the gaps between the sleepers and ballast to eliminate hanging sleepers.

2.1. Existing corrective countermeasures

The most common corrective countermeasure is tamping. During the process, sleepers are lifted to the required level and the ballast around the sleepers is packed into the void below the sleepers, either manually or by mechanical means (when possible). When the mechanised on-track tamping machines are used, vibrating tamping tines are introduced into the ballast on both sides of the sleeper. The vibration frequency is chosen so as to fluidise the ballast, which then is compacted inwards and upwards towards the bottom of the sleeper [41]. In case of some special structures, the tamping machines are difficult to employ. Tamping using manual or mechanised vibrating hammers is therefore necessary. During the process, sleepers are lifted by hydraulic rail jacks (sometimes sleepers are not lifted) and then four vibrating hammers are used, with consolidating heads opposing each other on both sides of the track. It should be noted that the manual tamping is prohibited in some countries (e.g. the Netherlands) due to health and safety rules. Since tamping does not add additional material to the track and make ballast less compacted, hanging sleepers will reappear at the relatively short time. The principle of tamping and operations using manual vibrating hammers [42] and mechanised vibrating hammers are shown in Fig. 4.

One way to fill the gap under hanging sleepers is to use hand-held stoneblower [41,43] or on-track stoneblower (when possible) [7,44–46]. The principle is first to lift the sleeper to the required level with minimum disturbances; and then to blow a pre-determined quantity of stones into the void under the sleeper using compressed air. The amount of the added stones is determined by the basis of the sleeper displacement before the stone blowing (using the void meter) [43]. The size of the blown stones is 14–20 mm, which is smaller than the ballast particle [41]. The principle of ballast blowing and a hand-held stoneblower are shown in Fig. 5 [42].

Another corrective countermeasure is to use the Automatic irregularity-correcting sleeper [47]. This kind of sleeper consists of a fibre-reinforced polymer sleeper and two automatic subsidence compensating devices under each rail. The automatic subsidence compensating device has two nested boxes (see Fig. 6(a)), which allows relative vertical movement. The inner box is connected to the rail through the sleeper, while the outer box is laid on the ballast. The inner box is filled with the (2 mm-diameter) granular material. When the differential settlement appears in the track, the outer box sinks together with the ballast. At the moment, the gap between the inner box and the outer box is filled with the granular material as shown in Fig. 6(b). Therefore, the differential settlement is compensated by the granular material as shown in Fig. 6(c).

2.2. Proposed corrective countermeasure

An innovative way to remove the gap under the hanging sleepers is by using adjustable fasteners which consist of two plastic wedges (shims) inserted between sleepers and rails (Fig. 7) instead of the rail pad. The height of the adjustable fastener can be changed by adjusting the position of the two wedges (shims) to fill the gap, which is 7–37 mm (i.e. the net adjustable height is 0–30 mm). When hanging sleepers appear, the height of the shims can be manually adjusted. As a result, the hanging sleepers can be restored to be fully supported by the ballast under. The principle of using adjustable fasteners is shown in Fig. 7(b) and (c). An example of the adjustable fastener used in the track is shown in Fig. 7(c). The stiffness of the shims (see Fig. 8(c)) has been tested in the laboratory of TU Delft [48] prior to the filed implementation as shown in Fig. 8, which follows the test procedures of rail fasteners stated in [49]. The load was applied by the hydraulic press machine (see Fig. 8(a)) and the displacements were measured by LVDTs (Linear Variable Differential Transformer, see Fig. 8(b)). During the test, the height of shims (adjusted height of the fasteners) was set to the maximum (37 mm including 30 mm adjusted height). The shims were installed in the fastener attached to an NS90 concrete sleeper and a section of UIC 54E1 rail. The test results show that the vertical stiffness of the shims is 8.02E8 N/m and no heavy visible damage was found after loading.

3. Experimental analysis

To study the effectiveness of the adjustable fasteners, they were tested on three transition zones in the track between Utrecht and Houten, the Netherlands. The natural ground in that region mainly consists of soft soil. According to the ground map of the location measured in 2012 [50], the natural ground of the measured lines is mostly clay, as shown in Fig. 9. A detailed field survey including Cone Penetration Tests and Vertical Seismic penetration Tests at a nearby location can be found in [2,37]. The tracks were newly constructed and no transition slabs were employed in the transition zones. Heavy traffic was expected on the tracks, including both passenger trains and freight trains. The change of the traffic amount was negligible during the whole measurement period. Since the fasteners are adjusted to fill the gaps under sleepers, the adjusted height equals the accumulated voiding, which can represent the degradation process of tracks at the moment. Therefore, the adjusted heights of the fasteners are recorded to analyse the track degradation.

3.1. Measurement set-up

The measurements were performed on the transition zones which consist of ballast tracks and slab tracks (the rails are directed fastened on metallic or concrete structures) [51]. The three (Embankment-Slab track-Embankment) transition zones are named Transition Zone A, B, and C, as shown in Fig. 10.

The adjustable fasteners had been installed on ten sleepers on both sides of slab tracks when the tracks were constructed. At that moment, the fasteners were set to their lowest position (i.e. adjusted height is 0 mm). The new tracks including the transition zones were levelled and aligned by tamping machines before the tracks went into service, as shown in Fig. 11.

The fasteners were adjusted after the 2-month operation and after the 5-month operation. During the adjustments, the fasteners were first unfixed (see Fig. 12(a)); then the rails were lifted to the required level by standard rail jacks (see Fig. 12(b)) or hydraulic rail jacks. After that, the fasteners were adjusted to the desired height by sliding shims. The

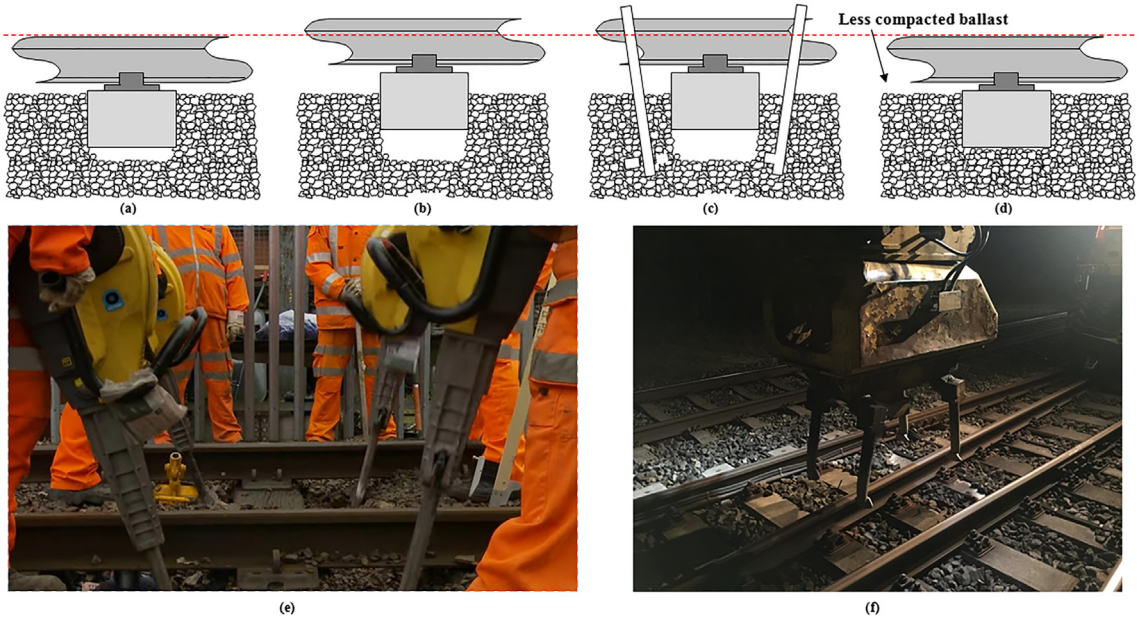

Fig. 4. Schematic diagram of tamping: (a)–(d) Working principle, (e) Operation using manual vibrating hammers [42], (f) Operation using mechanised vibrating hammers.

schematic diagram of using adjustable fasteners in transition zones are explained in Fig. 13. Since there was no operation specification for the adjustable fasteners, the adjustment mainly depended on the experience of the working staff. The operation for one side of a slab track (ten sleepers) required approximately fifteen minutes with three or four working staff. The adjusted heights of fasteners after two months and five months were recorded to analyse the development of the settlement in transition zones. It should be noted that due to practical reasons the fasteners on the embankment-slab track side of Transition Zone A were not possible to adjust after five months.

3.2. Measurement results

The adjusted heights of fasteners (accumulated voiding) of Transition Zone A, B, and C are shown in Figs. 14–16, respectively. It should be noted that since the adjusted height of all fasteners is 0 mm at 0 month, it is omitted in the figures. For convenience, the sleepers are numbered starting from the one closest to the slab track. The numbers are negative on the left side of the slab track (the embankment-slab track transition) and positive on the right (the slab track-embankment transition). The moving direction of the trains are indicated in the figures.

As it can be seen from Fig. 14–16, the settlement of ballast tracks appears after the 2-month operation where the maximal settlement values within 5 mm (in Transition zone C)-11 mm (in Transition zone B) can be found. The settlement is comparable with the measurement results in [2,10], where more than 10 mm settlement were also found after the 2-month operation. This is reasonable since both locations have the soft subsoil. The track settlement close to the slab track is higher in comparison with that farther from slab tracks. The settlement

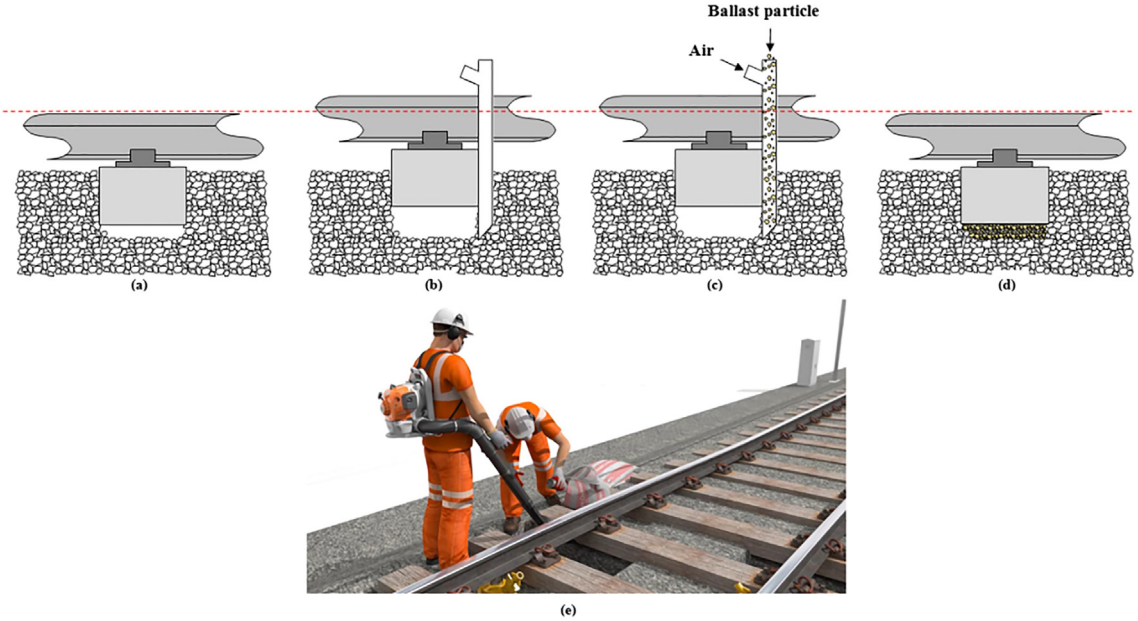

Fig. 5. Schematic diagram of stone blowing: (a)–(d) Working principle, (e) Demonstration from [42].

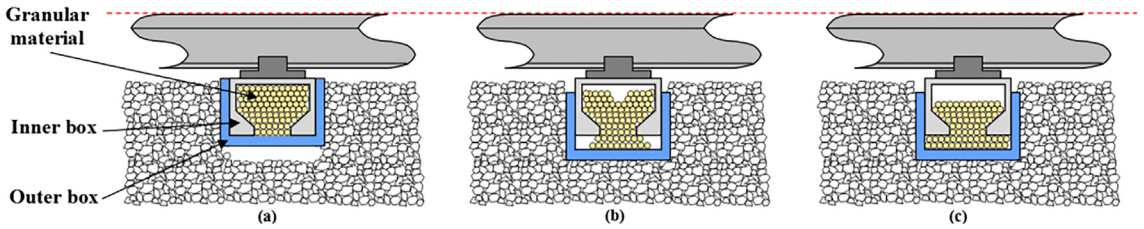

Fig. 6. Working principle of the Automatic irregularity-correcting sleeper.

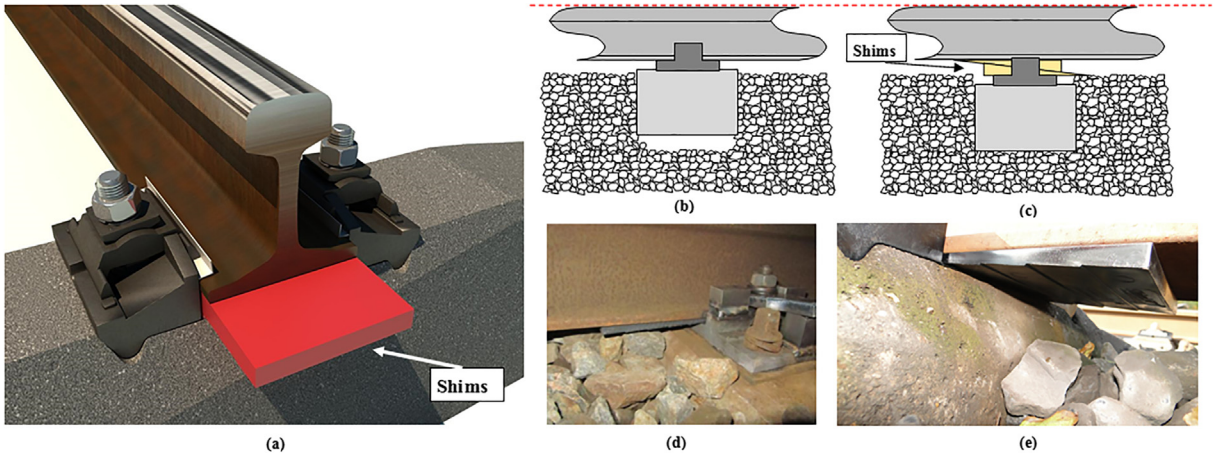

Fig. 7. Schematic diagram of Adjustable fastener: (a) Adjustable fastener, (b), (c) Working principle, (d), (e) Examples of the adjustable fastener used in the track.

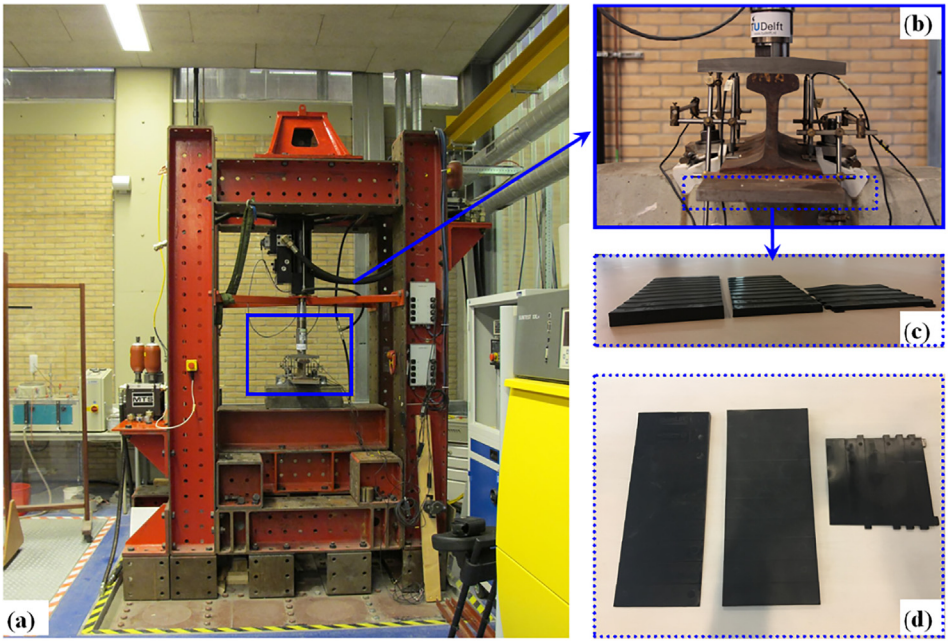

Fig. 8. Laboratory test of the shims: (a) Hydraulic press machine, (b) Zoom-in photo at the actuator with LVDTs, (c) Side view of the shims, (d) Top view of the shims.

reaches the largest amount at the 2nd or 3rd sleepers from the slab track (Sleeper ± 2, Sleeper ± 3); after that, it gradually reduces to 0 mm at the 8th or 9th sleepers (Sleeper ± 8, Sleeper ± 9). This is mainly because the ballast/subballast layer was not full stabilised before the operation, i.e. the rapid compaction process (Stage 1 in Fig. 2) happened. This confirms the theory of the appearance of the different settlement in transition zones which is explained in Section 1 that the settlement near engineering structures is much higher than that farther from engineering structures. It is also consistent with the measurement results in [52].

It should be noted that the settlement at the 1st sleeper is less than that at the 2nd or 3rd sleepers. It is because the rail is constrained by the slab track. As a result, the 1st sleeper has less movement under train loads and generate smaller impact to the ballast. In addition, the wheel forces are increased when the bogie is half on the slab track and half on the embankment, the distance of which corresponds to the 2nd or 3rd sleepers [18].

At the 2-month operation, the ballast tracks were compacted while the slab tracks were almost unchanged, which caused a differential settlement in the transition zones. If no corrective countermeasure was

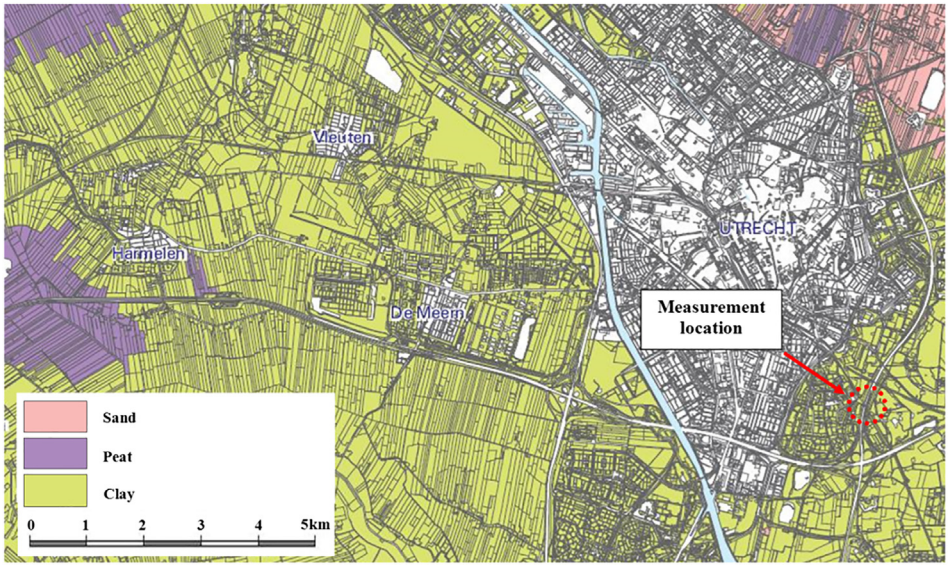

Fig. 9. Ground map of the measurement location.

implemented, the tracks in the transition zones would continue degrading due to the amplified dynamic wheel loads and ballast stress [20,53–57]. However, after filling the voiding using adjustable fasteners at the 2nd month, the growth rate of the settlement in ballast tracks was significantly reduced, which can be seen by comparing the accumulated settlement in the 0–2nd month and that in the 2nd–5th month in Figs. 14–16. Also, the measurement results of Transition Zone A-C (averaged settlement measured at the locations of the 1st to 4th sleepers to the slab track) are compared with the transition zone without adjustable fasteners (the settlement at 4 m from a culvert) from [10] in Fig. 17. As shown in Fig. 17, large settlements are found both in the transition zones with and without adjustable fasteners after the 2-month operation, which is mostly caused by the rapid compaction of ballast/subballast. However, there is also a relatively large settlement generated in the 2nd–5th month in the transition zone without adjustable fasteners, which accounts for 40% of the settlement in the 0–2nd month. On the contrary, the proportion is only within 7% (Transition Zone A)-19% (Transition Zone C) in the cases of the using the adjustable fasteners. It indicates that the adjustable fasteners reduce the growth rate of the settlement (i.e. degradation rate) in the transition zones.

4. Numerical analysis

Since the adjustable fasteners are proved to be effective in the field measurement, its effect on the dynamic behaviour of transition zones is analysed using the FE method.

Fig. 11. Tamping in a transition zone.

4.1. Introduction of FE model

The FE model used in the paper is based on the model proposed in [58] and further developed in [18,57]. In this study, it is tuned according to the measured transition zones. The model is pre-processed in ANSYS and solved in LS-DYNA. The modelling method and the parameters are briefly described here. The model consists of two ballast tracks and a slab track (in between), as shown in Fig. 18. When the railway vehicle moves from one ballast track to the other (from left to right), it is possible to analyse both the embankment-slab track and the

Fig. 10. Photographs of the measured transition zones.

Fig. 12. Adjustment of the fasteners.

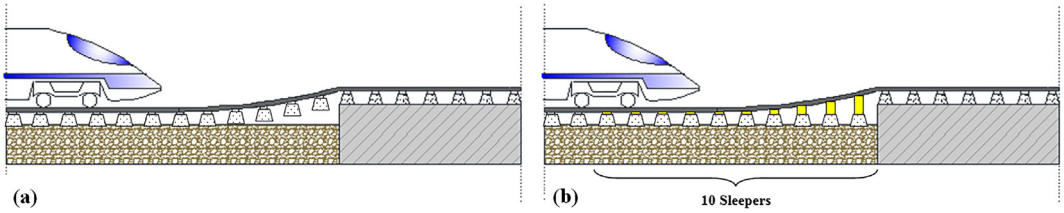

Fig. 13. Schematic diagram of using adjustable fasteners in transition zones.

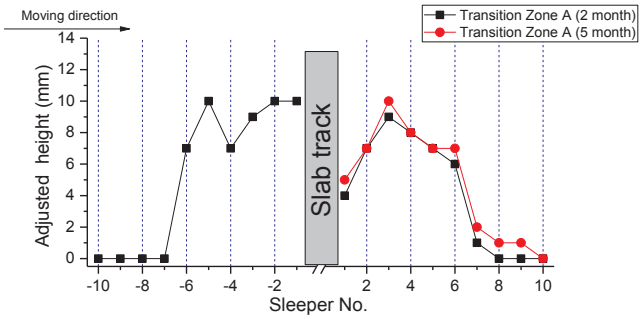

Fig. 14. Adjusted heights of the fasteners in Transition Zone A.

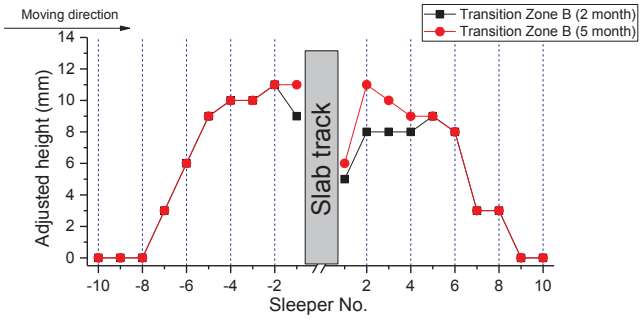

Fig. 15. Adjusted heights of the fasteners in Transition Zone B.

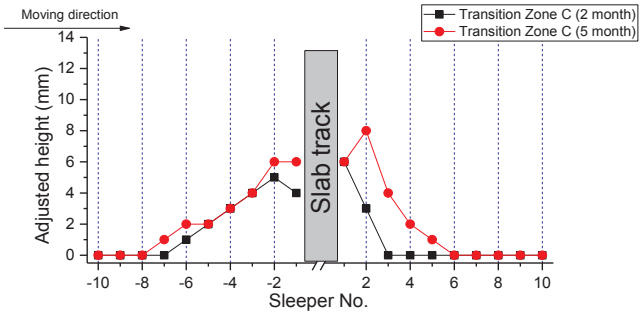

Fig. 16. Adjusted heights of the fasteners in Transition Zone C.

slab track-embankment transition with a single calculation. In the model, the 'slab track' is symbolical and not analysed to reduce calculation costs, because the purpose of the paper is to study the ballast track degradation in the transition zone rather than the slab track itself. The effect of the mortar layer [59] and the temperature [60] is not considered.

As the length of the ballast track is 48 m and the slab is 24 m, thereby, the total length of the transition zone is 120 m. The components of ballast tracks are rails, fasteners, sleepers, ballast, and subgrade. The rails are modelled by the beam elements with the cross-section and mass properties of the UIC54 rails. The adjustable fasteners are modelled by spring-damper elements which have bilinear material property. In compression, the elements can model elastic rail pads; and in tension, the elements can model the clamping effect of fasteners. In this way, hanging sleepers can be attached to rails, leaving gaps underneath.

Ballast, sleepers, and subgrade are modelled using the selective reduced integrated solid elements (element type 2 in LS-DYNA) with elastic material properties. This solid element assumes that the pressure is constant throughout the element to avoid pressure locking during nearly incompressible flow. The depth of ballast and subgrade layer is 0.3 m and 2 m, respectively.

The railway vehicle is a passenger vehicle, which is idealized as a multibody system consisting of one carbody, two bogies, and four wheelsets. The parameters of the vehicle are based on [61] and adapted to a Dutch passenger train [2,62]. The velocity of the vehicle is 144 km/h (standard operation velocity). Since the wheels are modelled as rigid bodies and rails as beam elements, the contact between the wheels and rails is the contact between the node at the wheel bottom and the beam, which is modelled using the Hertzian spring [43]. The stiffness is calculated according to Eq. (1).

$$k_H = \sqrt[3]{\frac{3E^2Q\sqrt{R_{wheel}R_{railprof}}}{2(1-\nu^2)^2}}, \tag{1}$$

where: E is the modulus of elasticity of the wheel and rail; ν is the Poisson's ratio; Q is the static vertical wheel load; R_{wheel} is the radius of the wheel; $R_{railprof}$ is the radius of the railhead [43,63]. The Hertzian spring is simplified by considering the static vertical wheel load, which follows [64]. It should be noted that the wheel-rail contact can be modelled more accurately by considering the dynamic wheel load

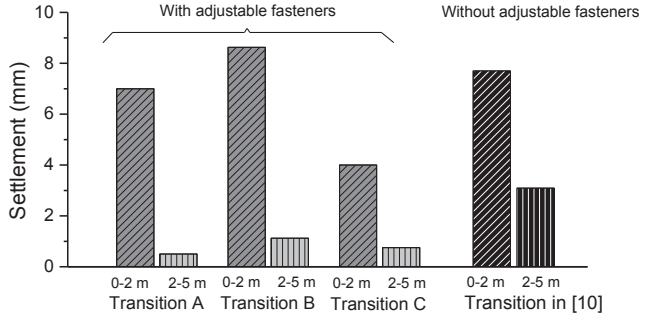

Fig. 17. Comparison between the settlement transition zones with and without adjustable fasteners.

(wheel-rail interaction force). However, the simplification is made due to the limitation of the calculation power.

The connection between sleepers and ballast is modelled by the Penalty-based contact [65] (surface to surface contact) in order to accurately present the spatial movement of sleepers and consequent ballast stresses. The Penalty-based contact employs the penalty method, which places normal interface springs between all penetrating nodes and the contact surface. The search for penetrations between the bottom surface of sleepers and the top surface of ballast is made for every time step during the calculation. In the case that the penetration happens, no force is added. When the penetration between contact surfaces has been found, a force proportional to the penetration depth is applied to resist and ultimately eliminate the penetration. The contact stiffness is determined by the minimum of the slave and master stiffness, which is the stiffness of the ballast in this case [66]. The ballast elements under one sleeper are treated as a part (see the mesh in Fig. 18). The same contact is also used for the vertical interfaces between part s of ballast elements. The friction coefficient is set as 0.75.

On the contrary, the Constraint-based contact [65] (tied contact) is used between the ballast and subgrade, and between the slab and the support layer. In the tied contact, the slave nodes are constrained to move with the master surface. The non-reflection boundaries [66] are applied to both ends of the model in order to reduce the wave reflection effect. The translation and rotation freedom of the nodes on the bottom of the subgrade and slab track are fixed. The material properties of the track components and the vehicle used in the model are suggested by [24,30,34,67–70] and tuned according to the field measurements described in [18]. The main parameters used in the model are collected in Table 1. It should be noted that the elastic modulus of the subgrade used in the model is most probably higher than the measured transition zones presented in Section 3, because the subgrade of the measured transition zones is clay (see Fig. 9). However, due to some practical reasons, the elastic modulus of the subgrade was not tested during the

Table 1
Material properties of the track components.

Parameter	Value
Sleeper elastic modulus (Pa)	3.65E + 10
Sleeper Poisson ratio	0.17
Sleeper density (kg/m^3)	2.50E + 3
Ballast elastic modulus (Pa)	1.20E + 08
Ballast Poisson ratio	0.25
Ballast density (kg/m^3)	1.80E + 3
Subgrade elastic modulus (Pa)	1.80E + 08
Subgrade Poisson ratio	0.250
Subgrade density (kg/m^3)	2.30E + 3
Concrete slab elastic modulus (Pa)	3.50E + 10
Concrete slab Poisson ratio	0.17
Concrete slab density (kg/m^3)	2.50E + 3
Support layer elastic modulus (Pa)	3.30E + 10
Support layer Poisson ratio	0.17
Support layer density (kg/m^3)	2.50E + 3
Fastener vertical (compression) stiffness (N/m)	1.20E + 8
Fastener vertical (compression) damping (N*s/m)	5.00E + 4
Fastener vertical (tension) stiffness (N/m)	1.20E + 11
Fastener vertical (tension) damping (N*s/m)	5.00E + 4
Primary suspension stiffness (N/m)	4.25E + 5
Primary suspension damping (N*s/m)	1.00E + 6
Secondary suspension stiffness (N/m)	4.68E + 5
Secondary suspension damping (N*s/m)	6.50E + 4
Secondary suspension bending stiffness (Nm/rad)	1.05E + 4
Distance between wheels (m)	2.5
Distance between axles (m)	20.0
Length of train body (m)	23.0
Axle load (t)	21.4
Carbody mass (t)	64.6
Bogie mass (t)	2.4

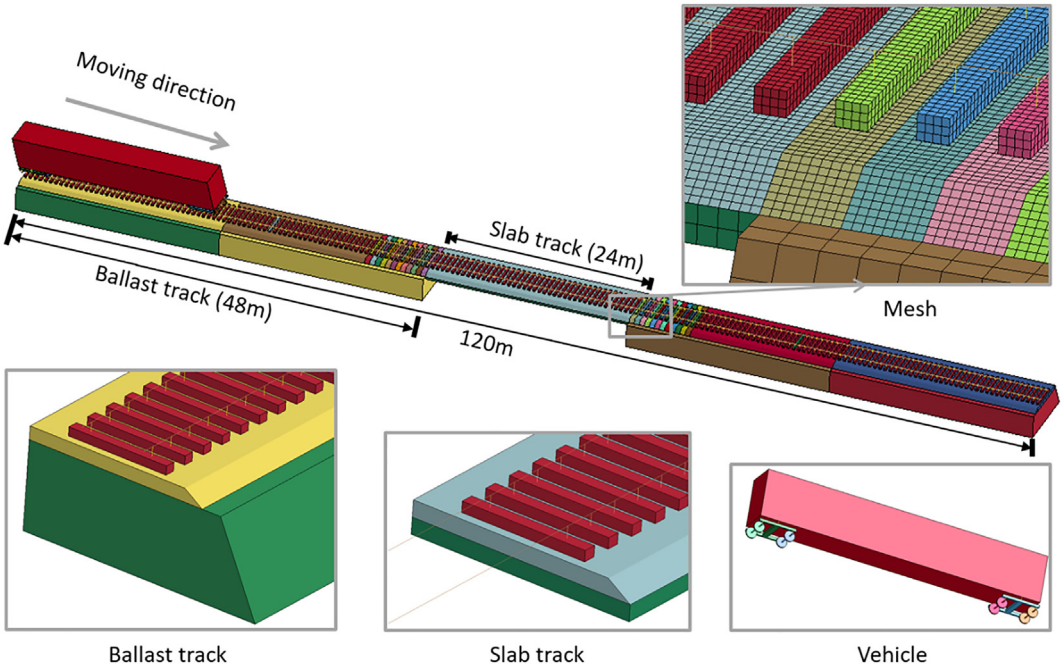

Fig. 18. FE model of track transition zones.

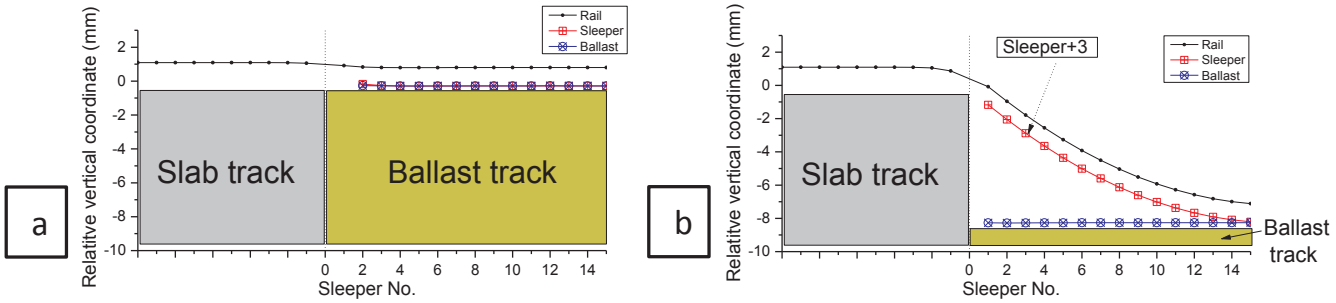

Fig. 19. Coordinates of track components before and after the implementation of the differential settlement: (a) Before, (b) After.

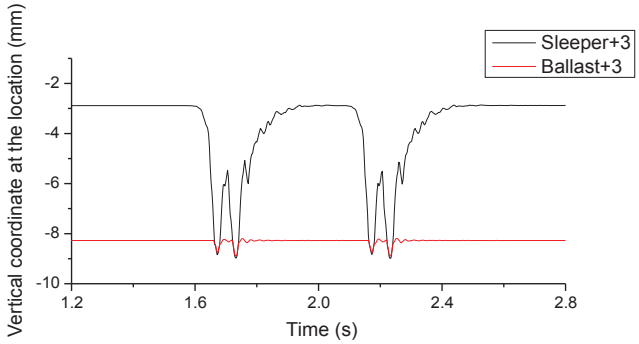

Fig. 20. Time history of vertical coordinate due to the passing vehicle at Sleeper + 3.

measurement. This will be discussed later.

The FE model considers the settlement of the ballast track due to the rapid compaction after the operation (settlement in Stage 1 as illustrated in Fig. 2). Since the exact settlement value is difficult to acquire, it is assumed to be equivalent to the adjusted height of the fasteners after 2 months. The maximal adjusted height varies from 5 mm (in Transition zone C) to 11 mm (in Transition zone B). As a result, the medium number 8 mm is adopted for the differential settlement value in the model. After that, the cases of 4 mm and 12 mm are also analysed in the parametric study. The rail longitudinal level, sleeper and ballast coordinates in the transition zone model before and after the implementation of the differential settlement are illustrated in Fig. 19.

At the equilibrium state of the model, due to separable contact between the sleepers and ballast, as well as the application of the gravity and the resistance of the rail, the gaps between the sleepers and ballast appear in the vicinity of the slab track, as shown in Fig. 19(b). The hanging distance of Sleeper + 1 is the highest and the hanging distance gradually reduces as the distance from the slab track increases. The hanging values of the sleepers are presented as the differences between the sleepers and ballast. The same situation is observed on the other side of the slab track. After the equilibrium state, the vehicle moves over the transition zone. The movement of a hanging sleeper (Sleeper + 3) is shown in Fig. 20.

The gap under the hanging sleeper is eliminated under train loads, where an increase of wheel-rail contact forces can be expected. When the sleepers contact the ballast, the penetrations between the bottom surface of the sleepers and the top surface of the ballast occur. The stress distribution in the ballast can be therefore calculated. Because the voids under sleepers are different depending on the location (see Fig. 19(b)), the stresses in the ballast elements under different sleepers also vary according to their locations.

In the transition zone using adjustable fasteners, the spring-damper elements are extended to compensate the gaps between the sleepers and ballast, as shown in Fig. 21. It should be noted that the stiffness and damping of adjustable fasteners are assumed to be same as normal fasteners (normal rail pads) and constant at various adjusted height. This simplification is made to reduce the computational expenses based on the findings that the effect of the differential settlement on dynamic responses is much larger in comparison with the stiffness variation [20,54,55,57]. The differential settlement is magnified in Fig. 21. In the actual case, the differential settlement (8 mm) is much smaller compared to the size of a sleeper (240 mm in height).

The study to find the optimal mesh sizes was performed prior to this study and it is not included due to the limited space. The model contains 675,686 nodes, 489,547 solid elements and 3612 beam elements. The time-step is 1.3E-5 s. The calculation takes around 14 h using a 4-core (I7) workstation with 4 High Parallel Computing (HPC).

4.2. Dynamic responses of transition zones with the adjustable fasteners

4.2.1. Wheel force

The calculated wheel forces of four wheelsets in the reference case and the adjustable fastener case are shown in Fig. 22. The wheel loads on the slab track are not considered in this study and therefore their responses are covered by the shaded area. The maximal wheel forces acting on ballast tracks are collected in Table 2.

Fig. 22 shows that the wheel loads are slightly vibrated around 105 kN, which is the static wheel load (210/2 = 105 kN); while they are increased considerably at both the embankment-slab track transition and the slab track-embankment transition in the reference case. This indicates the differential settlement lead to the amplification of wheel loads if no adjustable fastener is implemented, which is

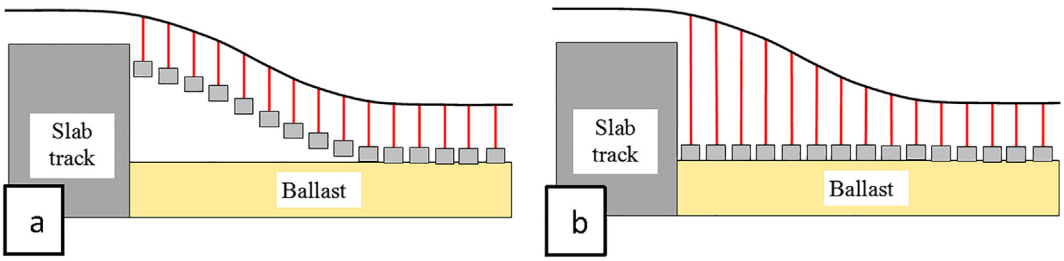

Fig. 21. Schematic diagram of the simulation of the countermeasure: (a) Reference, (b) Using adjustable fasteners. Fasteners are indicated by the red lines. (For interpretation of the references to colour in this figure legend, the reader is referred to the web version of this article.)

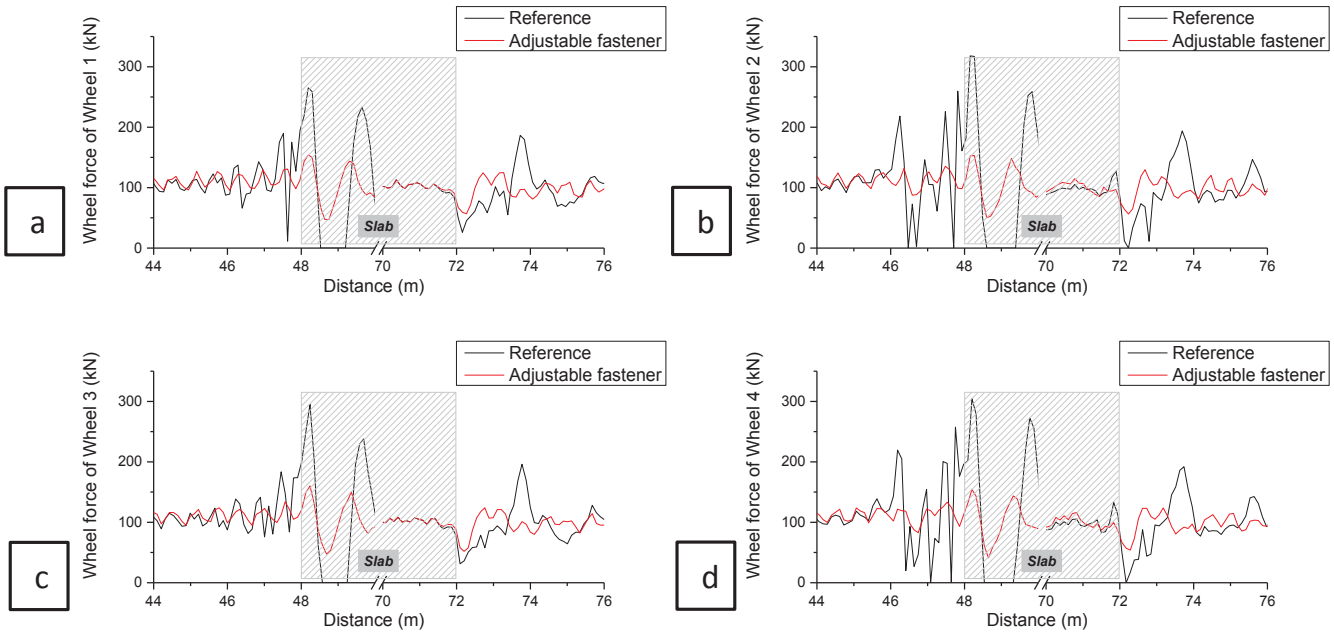

Fig. 22. Wheel-rail interaction force of four wheelsets: (a) Wheel 1, (b) Wheel 2, (c) Wheel 3, (d) Wheel 4. The wheel loads on the slab track are covered by the shaded area.

Table 2
Maximal wheel forces in the ballast track in transition zones from Fig. 22. The largest reduction is indicated as bold.

Wheel no.	Embankment-slab track transition			Slab track-embankment transition		
	Reference	Adjustable fastener	Reduction	Reference	Adjustable fastener	Reduction
1	190.0	130.8	45%	186.4	124.9	49%
2	259.8	135.4	92%	194.0	129.7	50%
3	183.6	133.9	37%	196.1	124.0	**58%**
4	257.6	133.3	**93%**	192.0	123.7	55%

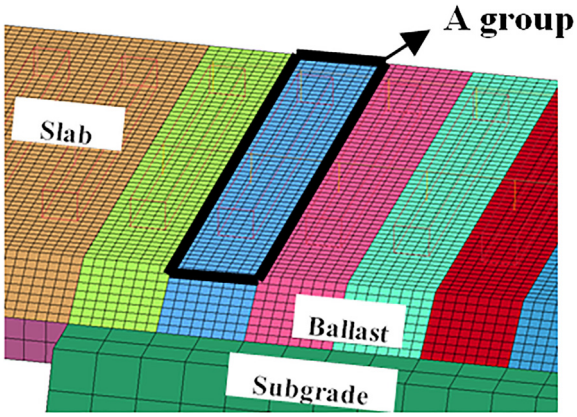

Fig. 23. Collecting method for ballast stresses. Red lines are sleeper frames. (For interpretation of the references to colour in this figure legend, the reader is referred to the web version of this article.)

consistent with [69]. It can also explain the track degradation in transition zones often reported in [7,9].

In [69], the dynamic responses of a train passing the transition zone (consisting of a ballast track with backfill and a long bridge) were studied. When the different settlement was 10 mm, the wheel load of Wheel 1 was increased on 50% the embankment and 64% on the engineering structure in comparison with the static load. In this study, the increases of the wheel load of Wheel 1 are 81% and 152%, respectively, which is comparable with the study in [69]. The discrepancy is mainly caused by the difference in contact settings and the constrain condition of the engineering structures (the slab track in this study is fixed by all the nodes on the bottom layer; while the bridge in [69] is fixed only at the ends of the bridge deck). As mention before, the elastic modulus of the subgrade of the measured transition zones are most probably lower than that used in the model. According to [8], the wheel-rail interaction force is increased when the elastic modulus of the subgrade reduces. Therefore, it can be inferred that the amplification of wheel-rail interaction forces is even higher in the case of the soft subgrade.

Comparing to the reference case, the wheel loads are reduced significantly when adjustable fasteners are in use (see Fig. 22 and Table 2). The reason is that the hanging sleepers in the transition zone are eliminated by the adjustable fasteners. This moment corresponds to the first adjustment of the fasteners in the measured transition zones after the 2-month operation (Section 3). The decrease of the amplified wheel loads (in Fig. 22 and Table 2) explains the substantial reduction of the track settlement growth rate in the measurement after using the adjustable fasteners.

4.2.2. *Ballast stress*

Since the ballast settlement depends on the ballast stress, the ballast stress in the transition zone is studied as well. It should be noted that the response of unbound granular materials like ballast is non-linear, which affects the calculated distribution of stresses inside the ballast. However, for the transient behaviour analysis in this study, the linear model is used as a first attempt, which is a typical approach, e.g. in [20,70], due to the limitation of the computational power. Moreover, the ballast bed in this model is assumed to be well compacted (after the rapid compaction). At the moment the sleeper contacting the top of the

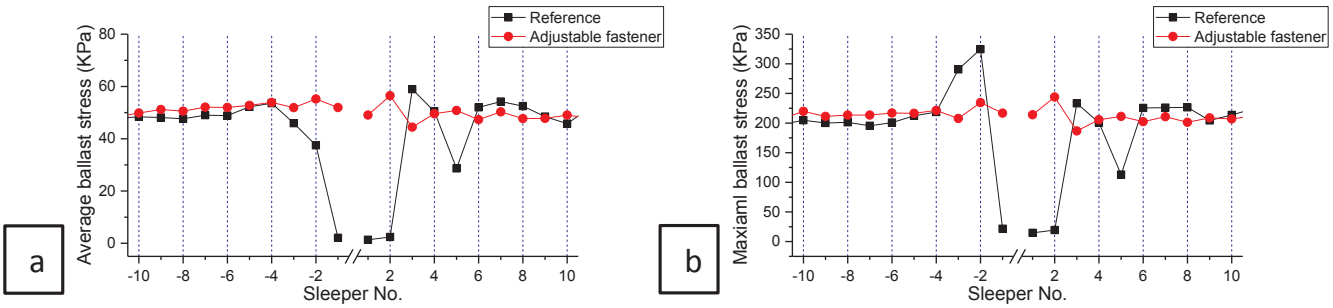

Fig. 24. Ballast stresses along the track: (a) Average; (b) Maximum.

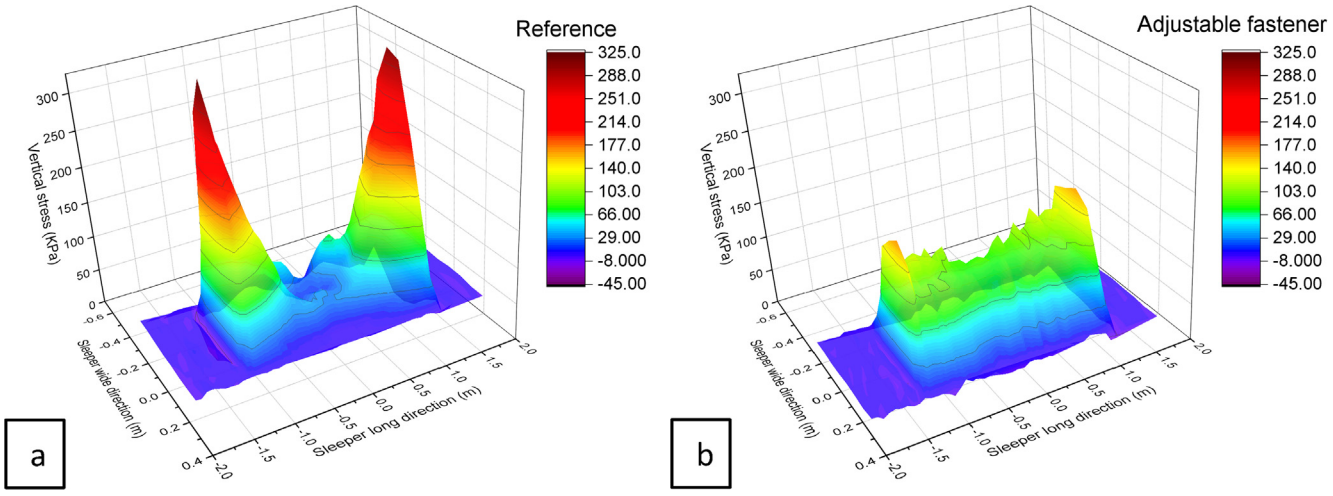

Fig. 25. Stress distribution in ballast under Sleeper-2: (a) Reference case, (b) Using adjustable fasteners.

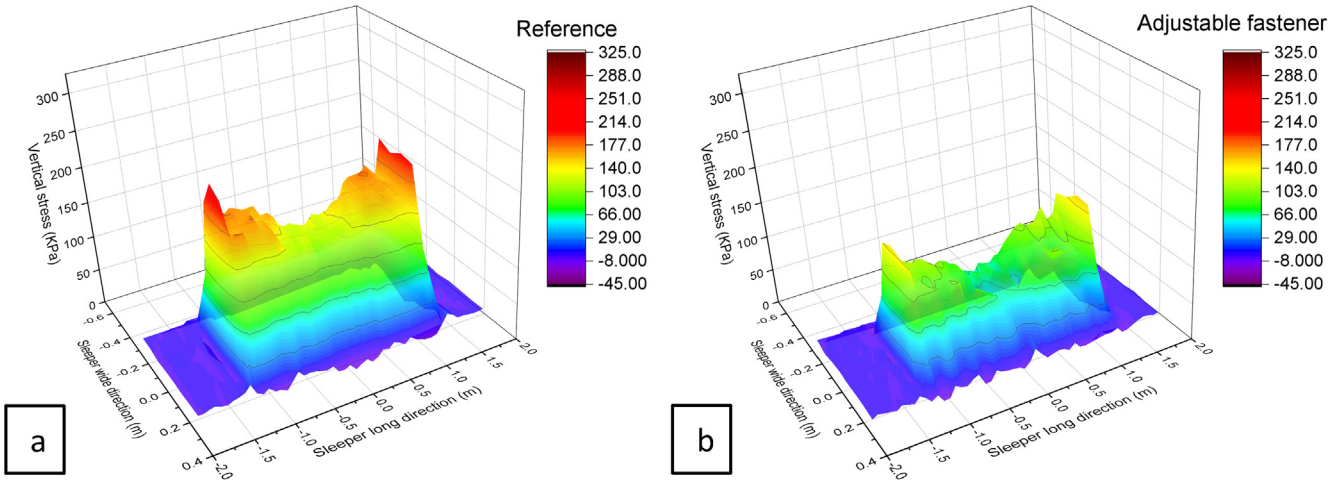

Fig. 26. Stress distribution in ballast under Sleeper + 3: (a) Reference case, (b) Using adjustable fasteners.

ballast, the ballast on the top can be simplified as the linear material. In order to analyse the ballast responses at the different locations, the ballast elements under one sleeper are considered as a group (unit), which are 416 elements ($52 * 8 = 416$, there are 8 elements on the wide side and 52 elements on the long side, see Fig. 23).

The vertical stresses in ballast under sleepers are analysed. The average and maximal stresses calculated for the ballast elements in each group along the track are shown in Fig. 24.

The maximal ballast stress is around 200 kPa at the location less affected by the slab track (e.g. Sleeper ± 10), which is reasonable in comparison with the measurement results in [71]. In [71], the ballast stress was measured during the passage of a coal train with 25t axle load. It is found that the maximal ballast stress was in the range between 160 and 230 kpa (with an outlier at 415 kPa due to a wheel-flat).

It also can be seen in Fig. 24(a) that, after using the adjustable fasteners, the average of ballast stresses are more evenly distributed along the track. In the reference case, the ballast stress closer to the slab track is lower than that at a greater distance from the bridge. It is because the hanging values of the sleepers are so large that the bending stiffness of rails resists the sleepers to fully contact the ballast. This confirms the finding from the measurement that the settlement at the 1st sleeper is less than that at the 2nd or 3rd sleepers. The stresses in rails at the moment can be expected high which will be discussed later.

Due to the poor support condition, the hanging sleepers can move

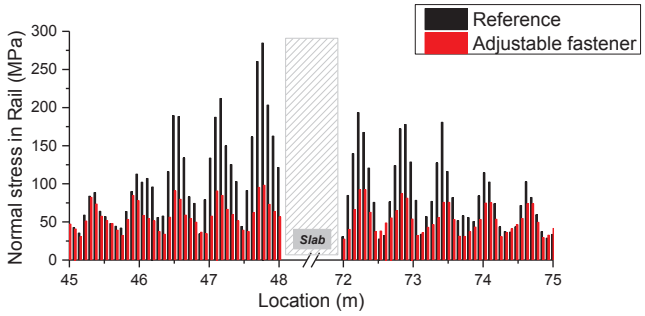

Fig. 27. Normal stresses in rails in the reference case and the adjustable fastener case.

irregularly, causing the stress concentrations in ballast, which can be proved by Sleeper-2 in Fig. 24(b). The maximal ballast stress reaches 325 kPa at Sleeper-2, which is approximately 60% higher comparing to the maximal ballast stress in a well-supported location. The stress distributions in ballast under Sleeper-2 in the two cases are shown in Fig. 25. The reduction of ballast stresses can be clearly seen from Fig. 25, where the maximal stress in ballast is reduced from 325 kPa to 235 kPa. A similar situation can also be found under Sleeper + 3, as shown in Fig. 26, where the maximal stress in ballast is reduced from 233 kPa to 187 kPa. Since the ballast stress is proportional to the settlement rate of ballast [72,73], the amplified stress may lead to the permanent settlement in ballast, which indicates the settlement (track degradation) in the transition zone may increase continuously if the adjustable fasteners are not implemented.

4.2.3. Rail stress

The maximal normal stresses in rails in the two cases are shown in Fig. 27. The rails are simulated by the beam elements with the length of 75 mm (eight elements in a sleeper space). As expected, the results show that the normal stresses in rails in the reference case are amplified near the slab track. When the adjustable fasteners are in use, the normal stresses are again decreased significantly. It shows the adjustable fasteners are also beneficial to rails.

To conclude, the adjustable fasteners are effective to reduce the amplification of the wheel forces, to achieve a better ballast stress distribution under the hanging sleepers, and to decrease the normal stresses in rails in transition zones.

4.3. Parametric study

4.3.1. Differential settlement value

Since the differential settlement value strongly depends on the material properties of tracks, the construction and operation condition, the differential settlement in transition zones may vary. To study the applicability of the adjustable fasteners, the transition zones with various differential settlements are modelled. Three values of the differential settlement are calculated, including 4 mm, 8 mm (the reference case in Section 4.2), and 12 mm. The wheel forces of Wheel 1 in three cases are compared in Fig. 28.

As it can be seen in Fig. 28, the wheel forces are increased as the differential settlement value grows near the slab track. It indicates that the adjustable fasteners should be used in the early stage of the differential settlement initiation. It should be noted that since the rapid compaction stage (Stage 1 of the settlement in Fig. 2) is somewhat inevitable, the fasteners should be adjusted as soon as the ballast track is compacted, namely, at the end of Stage 1 or the beginning of Stage 2. Stage 1 of the settlement ends at 0.5MGT according to [16]. Assuming five vehicles in a train, four trains in an operational hour, and fifteen operational hours in a day, it takes approximately twenty days to complete Stage 1 of the settlement.

The transition zones with adjustable fasteners in the cases of 4 mm and 12 mm are also studied. The wheel forces of Wheel 1 are shown in Fig. 29. It shows that the adjustable fasteners can significantly reduce the amplification of wheel forces in both cases, which indicates the applicability of the adjustable fasteners is relatively large.

4.3.2. Velocity

The effect of the adjustable fasteners is also studied in the cases of different velocities, including 90 km/h, 144 km/h (the reference case in Section 4.2) and 198 km/h. The wheel forces of Wheel 1 in three cases are shown in Fig. 30.

As expected, the wheel forces are amplified significantly near the slab track as the velocity increases, which can be seen in Fig. 30. The comparison of the wheel forces in the transition zones with and without adjustable fasteners is shown in Fig. 31.

Fig. 31 shows the wheel forces are reduced in both cases. A considerable reduction can be found in the case of 198 km/h, which is over 50%, from 350 kN to 165 kN. It indicates that the adjustable fasteners work in both low-velocity and high-velocity range and the benefit is more significant when the velocity is high.

5. Conclusions

The paper presents the experimental and numerical analysis of a corrective countermeasure-the adjustable fastener. Its working principle is to eliminate the gap under the hanging sleepers by adjusting the height of the fastener (relative position of two shims). The following conclusions can be drawn.

(1) Large differential settlements in the three transition zones were found after the 2-month operation, the maximum of which is ranged from 5 mm to 11 mm. The track settlements near the engineering structures (slab tracks) were much higher in comparison with that farther from the engineering structures.
(2) The growth rate of the settlement (i.e. degradation rate) of ballast

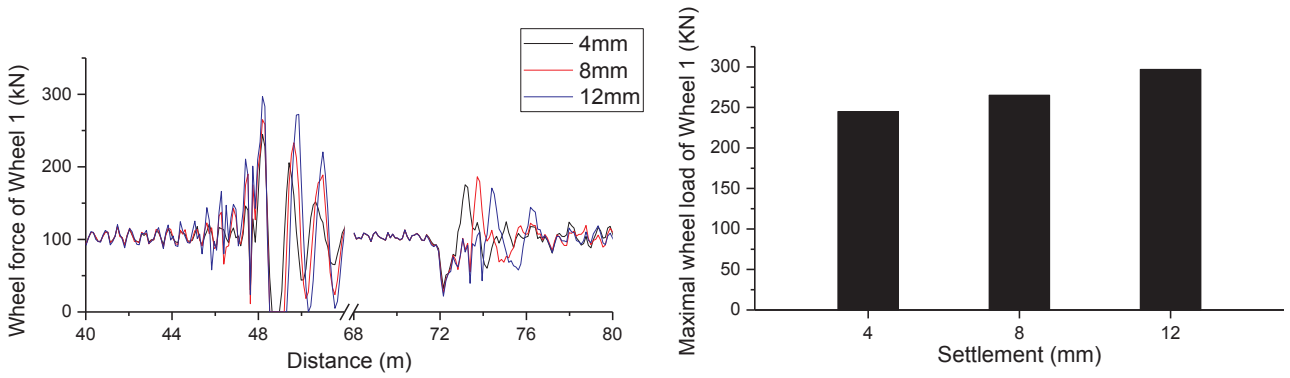

Fig. 28. Wheel force of Wheel 1 in three cases of settlement: (a) Time history; (b) Maximum.

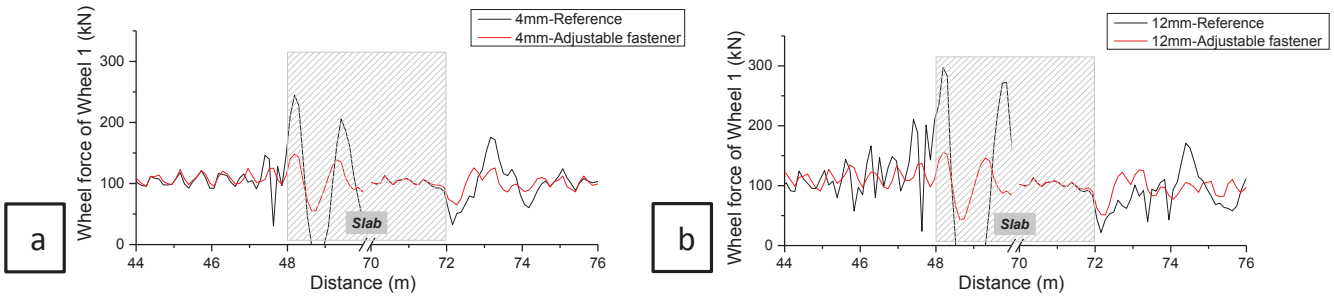

Fig. 29. Wheel forces of the transition zones using adjustable fasteners: (a) 4 mm differential settlement, (b) 12 mm differential settlement.

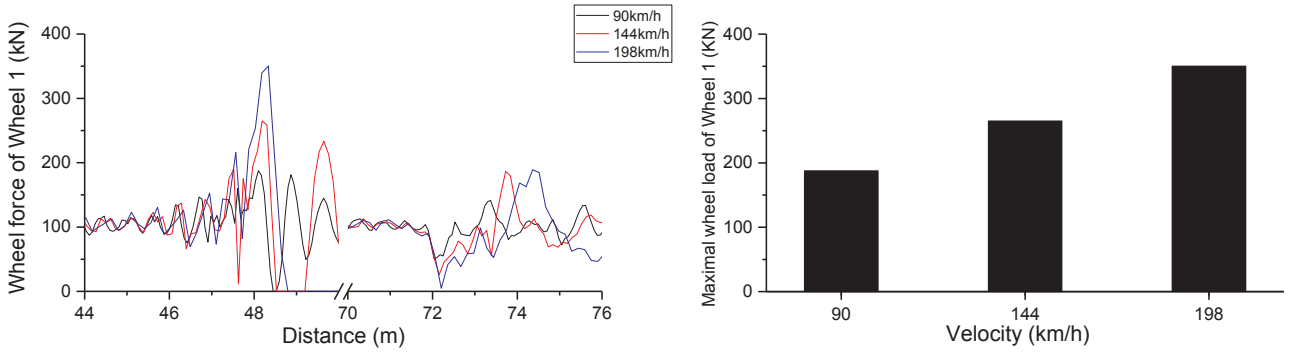

Fig. 30. Wheel force of Wheel 1 in three cases of velocity: (a) Time history; (b) Maximum.

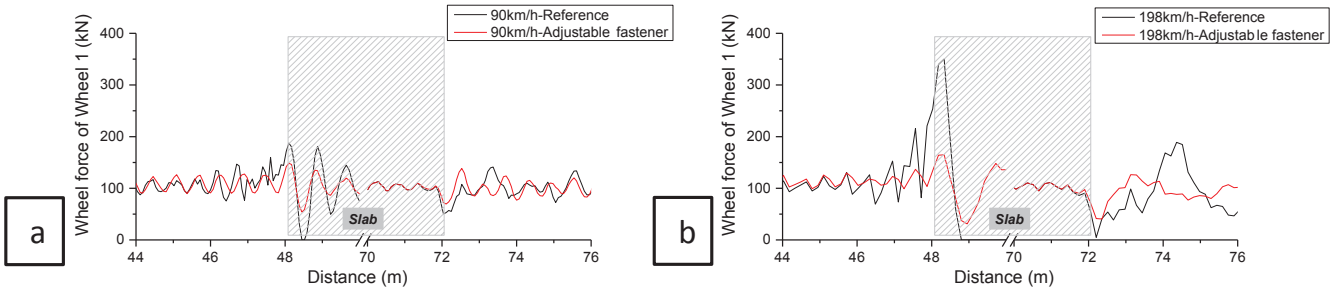

Fig. 31. Wheel forces of the transition zones using adjustable fasteners: (a) 90 km/h, (b) 198 km/h.

tracks is reduced significantly after the voiding in the track is filled with the adjustable fasteners.

(3) Numerical analysis shows that the adjustable fasteners are effective to reduce the amplification of wheel forces, achieve a better stress distribution in ballast, and decrease the normal stresses in rails in transition zones.

(4) The parametric studies show that the applicability of the adjustable fasteners is relatively wide. The adjustable fastener works effectively at both low-velocity and high-velocity and its benefit is more significant when the velocity is high.

(5) It is recommended that the fasteners should be adjusted once the ballast track is compacted.

Acknowledgement

The authors would like to sincerely thank Jelte Bos (from Movares Nederland B.V) for providing the technical details of the adjustable fasteners, measurement results and comments of the paper. The adjustable fasteners mentioned in the paper is named ShimLift®, developed by Movares Nederland B.V together with BAM Infra Rail BV, and produced by Kampa-International BV. The authors would like to thank Jan Moraal (from TU Delft) for providing the laboratory test results of the adjustable fasteners. The authors would like to thank Network Rail Co. for providing related materials. The authors are very grateful to all reviewers for their thorough reading of the manuscript and their constructive comments.

References

[1] Li D, Otter D, Carr G. Railway bridge approaches under heavy axle load traffic: problems, causes, and remedies. Proc Inst Mech Eng, Part F: J Rail Rapid Transit 2010;224(5):383–90.

[2] Zuada Coelho B. Dynamics of railway transition zones in soft soils [Doctoral dissertation]; 2011.

[3] Varandas JN, Hölscher P, Silva MAG. Dynamic behaviour of railway tracks on transitions zones. Comput Struct 2011;89(13–14):1468–79.

[4] Hölscher P, Meijers P. Literature study of knowledge and experience of transition zones, in Delft: report; 2007.

[5] Sasaoka C, Davis D. Long term performance of track transition solutions in revenue service. Technology Digest TD-05-036, Transportation Technology Center. Inc., Association of American Railroads; 2005.

[6] Hyslip JP, Li D, McDaniel C. Railway bridge transition case study. In: Bearing capacity of roads, railways and airfields. 8th International Conference (BCR2A'09); 2009.

[7] Stark TD, Wilk ST. Root cause of differential movement at bridge transition zones. Proc Inst Mech Eng, Part F: J Rail Rapid Transit 2015.

[8] Nicks JE. The bump at the end of the railway bridge [Doctoral dissertation]. Texas A &M University; 2009.

[9] Li D, Davis D. Transition of railroad bridge approaches. J Geotech Geoenviron Eng 2005.

[10] Coelho B, et al. An assessment of transition zone performance. Proc Inst Mech Eng, Part F: J Rail Rapid Transit 2011;225(2):129–39.

[11] Paixao A, Fortunato E, Calcada R. Design and construction of backfills for railway track transition zones. Proc Inst Mech Eng, Part F: J Rail Rapid Transit

2013;229(1):58–70.
[12] Sato Y. Japanese studies on deterioration of ballasted track. Veh Syst Dyn 1995;24(sup1):197–208.
[13] Shenton M. Ballast deformation and track deterioration. Track Technol 1985:253–65.
[14] Indraratna B, Ionescu D, Christie HD. Shear behaviour of railway ballast based on large scale triaxial testing. J Geotech Geoenviron Eng 1998:439–49.
[15] Varandas JN, Hölscher P, Silva MAG, A settlement model for ballast at transition zones. In: Proceedings of the Tenth International Conference on Computational Structures Technology; 2010.
[16] Selig ET, Waters JM. Track geotechnology and substructure management. Thomas Telford; 1994.
[17] Gerber U, Fengler W. Setzungsverhalten des Schotters [in German]. ETR. Eisenbahntechnische Rundschau 2010;59(4):170–5.
[18] Wang H, Markine V. Analysis and improvement of the dynamic track behaviour in transition zone. In: Loizos et al., editors. Tenth international conference on the bearing capacity of roads, railways and airfields. Athens, Greece: Taylor & Francis Group, London; 2017.
[19] Wang H, et al. Analysis of the dynamic behaviour of a railway track in transition zones with differential settlement. In: 2015 Joint Rail Conference, San Jose, California, USA, 2015; 2015. p. 7.
[20] Banimahd M, et al. Behaviour of train–track interaction in stiffness transitions. Proc ICE – Transp 2012;165(3):205–14.
[21] Lundqvist A, Dahlberg T. Load impact on railway track due to unsupported sleepers. Proc Inst Mech Eng, Part F: J Rail Rapid Transit 2005;219(2):67–77.
[22] Sañudo R, Markine V, Dell'Olio L. Optimizing track transitions on high speed lines. IAVSD2011; 2011.
[23] Gallego Giner I, López Pita A. Numerical simulation of embankment–structure transition design. Proc Inst Mech Eng, Part F: J Rail Rapid Transit 2009;223(4):331–43.
[24] Insa R, et al. Analysis of the influence of under sleeper pads on the railway vehicle/track dynamic interaction in transition zones. Proc Inst Mech Eng, Part F: J Rail Rapid Transit 2011;226(4):409–20.
[25] Alves Ribeiro C, et al. Under sleeper pads in transition zones at railway underpasses: numerical modelling and experimental validation. Struct Infrastruct Eng 2014;11(11):1432–49.
[26] Dahlberg T. Railway track stiffness variations-consequences and countermeasures. Int J Civ Eng 2010;8(1).
[27] Shahraki M, Warnakulasooriya C, Witt KJ. Numerical study of transition zone between ballasted and ballastless railway track. Transp Geotech 2015;3:58–67.
[28] Sañudo R, et al. Track transitions in railways: a review. Constr Build Mater 2016;112:140–57.
[29] Puppala AJ, et al. Recommendations for design, construction, and maintenance of bridge approach slabs: Synthesis report, in Rep. No. FHWA/TX-09/6022; 2009.
[30] Shan Y, Albers B, Savidis SA. Influence of different transition zones on the dynamic response of track–subgrade systems. Comput Geotech 2012;48:21–8.
[31] Kaewunruen S. Dynamic responses of railway bridge ends: a systems performance improvement by application of ballast glue/bond.
[32] Horníček L, et al. An investigation of the effect of under-ballast reinforcing geogrids in laboratory and operating conditions. Proc Inst Mech Eng, Part F: J Rail Rapid Transit 2010;224(4):269–77.
[33] Woldringh RF, New BM. Embankment design for high speed trains on soft soils.
[34] Read D, Li D. Design of track transitions. TCRP Research Results Digest 79; 2006.
[35] Sasaoka CD, Davis DD. Implementing track transition solutions for heavy axle load service. In: AREMA 2005 Annual Conference. Chicago; 2005.
[36] Namura A, Suzuki T. Evaluation fo countermeasures against differential settlement at track transitions. QR RTRI 2007;48(3).
[37] Varandas JN. Long-term behaviour of railway transitions under dynamic loading application to soft soil sites [Doctoral dissertation]; 2013.
[38] Coelho Z. Dynamics of railway transition zones in soft soils; 2011.
[39] Markine V, Wang H, Shevtsov I. Experimental analysis of the dynamic behaviour of a railway track in transition zones. In: Proceedings of the Ninth International Conference on Engineering Computational Technology, P. Iványi and B.H.V. Topping, (Editors), Civil-Comp Press, Stirlingshire, United Kingdom, paper 3, 2014; 2014.
[40] Le Pen L, et al. The behaviour of railway level crossings: insights through field monitoring. Transp Geotech 2014;1(4):201–13.
[41] Claisse P, Calla C. Rail ballast: conclusions from a historical perspective. London: Published for the Institution of Civil Engineers by Thomas Telford Services; 1992-.
[42] NetworkRail. Pictures from Network Rail; 2016. Available from: https://www.networkrail.co.uk/.
[43] Esveld C. Modern railway track vol. 385. The Netherlands: MRT-productions Zaltbommel; 2001.
[44] Tutumluer E, et al. Investigation and mitigation of differential movement at railway transitions for US high speed passenger rail and joint passenger/freight corridors. In: 2012 Joint Rail Conference. American Society of Mechanical Engineers; 2012.
[45] Stark TD, Wilk ST, Sussmann TR. Evaluation of tie support at transition zones. Transp Res Rec: J Transp Res Board 2015;2476:53–8.
[46] Anderson WF, Key AJ. Model testing of two-layer railway track ballast. J Geotech Geoenviron Eng 2000;126(4):317–23.
[47] Muramoto K, Nakamura T, Sakurai T. A study of the effect of track irregularity prevention methods for the transition zone between different track structures. Quart Rep RTRI 2012;53(4):211–5.
[48] Moraal J. Dynamische beproeving ShimLift bevestiging op NS90 ligger, in TU Delft Report. TU Delft; 2013.
[49] CEN(European-Committee-for-Standardization), Railway applications – Track – Test methods for fastening systems - Part 9: Determination of stiffness; 2009. p. 30.
[50] Wageningen U, and Research, Dutch soil map, part of the Fertilizer Act 2012 – WUR.
[51] Bos J, Jansen J. Evaluation of ShimLift pilots Evaluating; 2013.
[52] Wang H, Markine V, Liu X. Experimental analysis of railway track settlement in transition zones. Proc Inst Mech Eng, Part F: J Rail Rapid Transit 2017: 0954409717748789.
[53] Lei X, Mao L. Dynamic response analyses of vehicle and track coupled system on track transition of conventional high speed railway. J Sound Vib 2004;271(3–5):1133–46.
[54] Banimahd M, Woodward PK. 3-Dimensional finite element modelling of railway transitions. In: 9th International Conference on Railway Engineering; 2007.
[55] Zhai WM, True H. Vehicle-track dynamics on a ramp and on the bridge: simulation and measurement. Vehicle Syst Dyn 1999;33(Supply): 11.
[56] Plotkin D, Davis D. Bridge approaches and track stiffness; 2008.
[57] Wang H, et al. Analysis of the dynamic behaviour of a railway track in transition zones with differential settlement. In: 2015 Joint Rail Conference, San Jose, California, USA, March 2015; 2015. p. 7.
[58] Wang H, Markine VL, Shevtsov IY. The analysis of degradation mechanism in track transition zones using 3D finite element model. In: Pombo J, editor. Proceedings of the Second International Conference on Railway Technology: Research, Development and Maintenance, Civil-Comp Press, Stirlingshire, United Kingdom, paper 227, 2014; 2014. http://dx.doi.org/10.4203/ccp.
[59] Chen R, et al. Degradation mechanism of CA mortar in CRTS I slab ballastless railway track in the Southwest acid rain region of China-Materials analysis. Constr Build Mater 2017;149:921–33.
[60] Chen R, et al. The continuous-slab-track coupling laws between the bridge and track under temperature loads. J Rail Eng Soc 2017;34(3):15–21.
[61] Iwnick S. Manchester benchmarks for rail vehicle simulation. Veh Syst Dyn 1998;30(3–4):295–313.
[62] Wan C, Markine VL, Shevtsov IY. Improvement of vehicle–turnout interaction by optimising the shape of crossing nose. Veh Syst Dyn 2014;52(11):1517–40.
[63] Knothe K, Grassie S. Modelling of railway track and vehicle/track interaction at high frequencies. Veh Syst Dyn 1993;22(3–4):209–62.
[64] Paixão A, Fortunato E, Calçada R. Transition zones to railway bridges: track measurements and numerical modelling. Eng Struct 2014;80:435–43.
[65] Hallquist JO. LS-DYNA keyword user's manual. Livermore, CA: LSTC Co.; 2007.
[66] Hallquist JO. LS-DYNA theory manual. vol. 3. Livermore, CA: Livermore Software Technology Corporation; 2006. p. 25–31.
[67] Oregui M, Li Z, Dollevoet R. An investigation into the modeling of railway fastening. Int J Mech Sci 2015;92:1–11.
[68] Nguyen Gia K, Goicolea Ruigómez JM, Gabaldón Castillo F. Dynamic effect of high speed railway traffic loads on the ballast track settlement. Congresso de Métodos Numéricos em Engenharia; 2011.
[69] Paixao A, Fortunato E, Calcada R. A numerical study on the influence of backfill settlements in the train/track interaction at transition zones to railway bridges. Proc Inst Mech Eng, Part F: J Rail Rapid Transit 2015.
[70] Shi J, et al. Measurements and simulation of the dynamic responses of a bridge-embankment transition zone below a heavy haul railway line. Proc Inst Mech Eng, Part F: J Rail Rapid Transit 2012;227(3):254–68.
[71] Indraratna B, et al. Field assessment of the performance of a ballasted rail track with and without geosynthetics. J Geotech Geoenviron Eng 2010;136(7):907–17.
[72] Sato Y. Optimization of track maintenance work on ballasted track. In: Proceedings of the World Congress on Railway Research (WCRR'97), B; 1997.
[73] Dahlberg T. Some railroad settlement models—a critical review. Proc Inst Mech Eng, Part F: J Rail Rapid Transit 2001;215(4):289–300.